A Study on the Characteristics of Fracture Resistance Curve of Ferritic Steels

Chang-Sung Seok* and Soo-Yong Kim**

(*Received May 3, 1999*)

Fracture resistance (J-R) curves are used for elastic-plastic fracture mechanics analyses. The specimen geometry and the reversed cyclic loading affect the fracture resistance (J-R) curve. On the specimen geometry, The effects of specimen size, plane size, specimen thickness, side grooving and crack length were studied. On the reversed cyclic loading, the effects of load ratio and incremental plastic displacement were studied. The results revealed that the J-R curves increased with increasing plane size and decreased with increasing a/W and the J-R curves decreased with decreasing the load ratio and the incremental plastic displacement, respectively.

Key Words: Fracture Resistance Curve, Constraint Effect, Reversed Cyclic Loading, Load Ratio, Incremental Plastic Displacement, Strain Hardening, Hardness Test, ABI Test, Crack Opening.

1. Introduction

The crack stability should be evaluated and confirmed prior to accept the Leak-Before-Break (LBB) design concept which eliminates the postulation of protective design activity against the unbalanced dynamic stroke at the piping break situation in nuclear power plant. The first step of evaluating the crack stability is to perform piping stress analysis to get critical points, where imaginary crack position is determined. The size of this postulated crack is determined from the leakage detecting abilities of the general nuclear power plants. With this virtual crack and its location, the piping system should withstand the most severe loading conditions that can happen in nuclear power plants.

In order to perform Leak-Before-Break analyses of nuclear piping systems, fracture resistance curves for concerned materials are required. The fracture resistance (J-R) curve was affected by the constraint effects (Kirk, et al. 1993; Theiss, et al. 1993; Joyce, et al. 1993) by means of variation of specimen dimension (size, thickness, plane size, normalized crack length, side groove and etc.) and the load history effects (Scott, et al. 1994; Wilkowski, et al. 1994; Miura, et al. 1997; Miura, Fujioka, et al. 1993; Choi 1995, Seok, et al. 1998) by means of load ratio and incremental plastic displacement. A major objective of this paper is to evaluate the variation of J-R curves as the constraint and load history variation of specimen.

* School of Mechanical Engineering, Sungkyunkwan University, 300 Chunchun-dong Changan--ku, Suwon, 440-746, Korea.

** School of Mechanical Engineering, Sungkyunkwan University, Suwon, Korea.

2. Fracture Toughness Test

The fracture toughness tests on cyclic loading was performed on the basis of the single specimen method specified in the ASTM E813 (1996) and E1152 (1996) for static fracture testing. To produce the plane-strain condition, pre-cracked CT specimens were 10% side grooved on each side with an edge angle of 45°. A servo-hydraulic computer controlled material testing system was used.

2.1 Specimen geometry varying test

The unloading compliance test procedure was

used in calculating the amount of crack growth. Compact tension specimens were prepared as specified in the ASTM E813-89 A2.1. The crack length to width ratio, a/W, was set to 0.55 for all specimens except for the specimens used for the investigation on the change of a/W. Test specimens used for the study on the effect of a/W were prepared by changing the a/W from 0.25 to 0.85. Four different compact tension specimens ranging from 0.5T (thickness: 12.7 *mm*) to 2T (thickness: 50.8 *mm*) were prepared to investigate the effect of specimen size. In order to investigate the effect of plane size, three different compact tension specimens were designed. The thickness was fixed to 25.4 *mm* and only the width was changed from 50.8 *mm* to 152.4 *mm*. The effect of specimen thickness was studied with 4 different specimen configurations. The specimen width was set to 101.6 *mm*, and the thickness was changed from 12.7 *mm* to 50.8 *mm*. In order to observe the effect of a/W, a total of 20 compact tension specimens were prepared. The size was fixed to 1T-CT, and a/W was changed from 0.25 to 0.85. For $a/W=0.45$ and 0.65, nsn-side-grooved specimens were also prepared. Two specimens were prepared for each configuration to ensure the test repeatability.

2.2 Reversed cyclic loading test

The DCPD method was used for measuring crack length and crack propagation. Firstly, the crack initiation displacement (δ_i) was obtained from the load-line displacement vs. potential drop (voltage) curve at monotonic loading condition. In this paper, the average value of crack initiation displacement determined under the monotonic loading was 1.92 *mm*. This crack initiation displacement was used for a criterion in determining the number of the reversed cyclic loading for the fracture resistance tests. In order to evaluate the effect of cyclic loading, the experiments were conducted at quasi-static loading rates with the load ratio (P_{min}/P_{max}, hereafter R) ranging from -1 to 1 and incremental plastic displacement (δ_{cycle}/δ_i, hereafter IPD) ranging from 1/40 to 1/5. In these tests, only the load ratio was varied for 7 different values covering

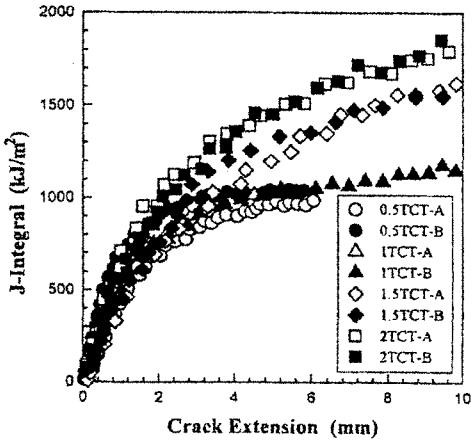

Fig. 1 Effect of Specimen Size on the Fracture Resistance Curve of SA515 Gr.60 Steel.

monotonic loading ($R=1$), $R=0.5$, $R=0$, $R=-0.3$, $R=-0.6$, $R=-0.8$, and $R=-1$ with a fixed normalized incremental plastic displacement of $\delta_{cycle}/\delta_i=0.1$. The experiments were also conducted at quasi-static loading rates and the incremental plastic displacement, δ_{cycle}/δ_i, was set to 5 different values of 1/5, 1/10, 1/20, 1/30, and 1/40 with a fixed load ratio of -1.

3. Effect of Specimen Configuration

3.1 Specimen size

The resulting J-R curves from eight specimens with different sizes are shown in Fig. 1. Except for a 2T-CT (thickness: 50.8 *mm*) specimen, J-R curves are very close until the crack extension reaches 3 *mm*. While all 0.5T-CT (thickness: 12.7 *mm*) and 1T-CT (thickness: 25.4 *mm*) specimens produced the same trend for the entire crack extension, 1.5T-CT (thickness: 38.1 *mm*) and 2T-CT specimens resulted higher J-integral values with crack extension over 3 *mm*. Since the plasticity development at the crack ligament is relatively larger for 0.5T specimens than other specimens, 0.5T specimens showed full plastic deformation at the crack tip with a crack extension of 3 *mm*. Larger specimens showed more energy absorption after the crack extension passed 3 *mm*.

3.2 Plane size

Figure 2 shows the resulting J-R curves from

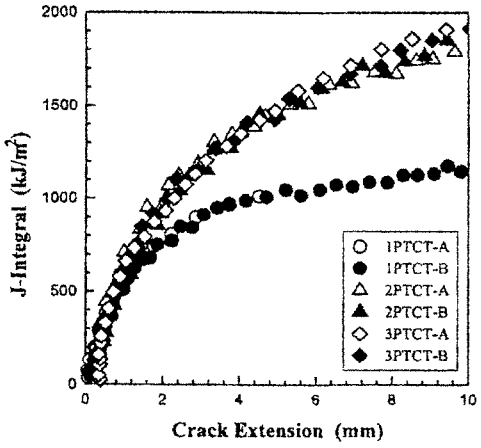

Fig. 2 Effect of Plane Size on the Fracture Resistance Curve of SA515 Gr.60 Steel.

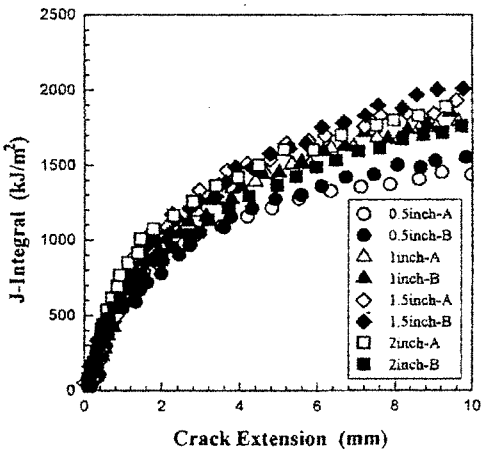

Fig. 3 Effect of Thickness on the Fracture Resistance Curve of SA515 Gr.60 Steel.

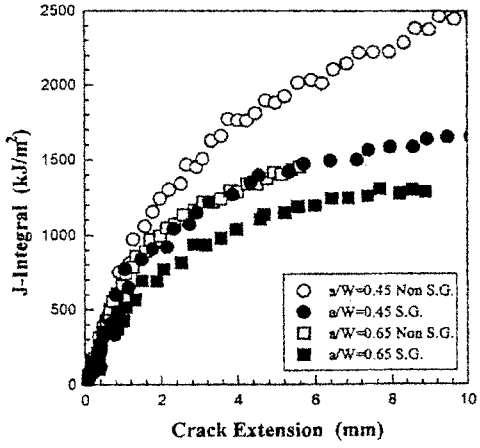

Fig. 4 Effect of Side Grooving on the Fracture Resistance Curve of SA515 Gr.60 Steel.

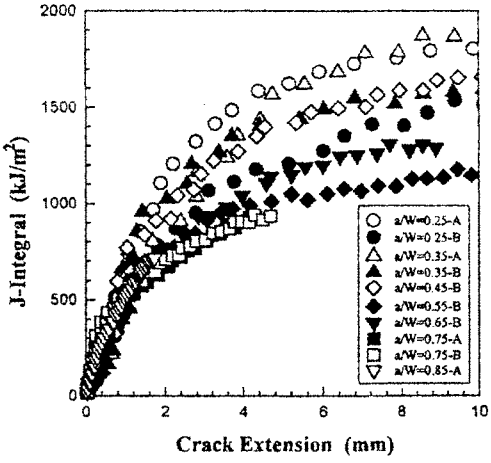

Fig. 5 Effect of Crack Length on the Fracture Resistance Curve of SA515 Gr.60 Steel.

various plane size specimens. It is clear that 2PT-CT (width: 101.6 *mm*) and 3PT-CT (width: 152.4 *mm*) specimens showed much higher J-R curves than those from 1PT-CT (width: 50.8 *mm*) specimens after the crack extension passed 1 *mm*. The difference increases with increasing crack extension, and the J-integral values for 2PT-CT and 3PT-CT specimens at 5 *mm* crack extension were about 40% higher than 1PT-CT specimens.

3.3 Specimen thickness

Figure 3 shows J-R curves obtained from various thickness specimens ranging from 12.7 *mm* (0.5 *inch*) to 50.8 *mm* (2 *inch*). All of the specimens were side grooved. No significant difference was observed for various thickness specimens as shown in Fig. 3.

3.4 Side grooving

Figure 4 shows a comparison between the side-grooved specimens and the non-side-grooved specimens. Since the side groove is designed to remove shear-lips which increases fracture toughness, non-side-grooved specimens resulted in much higher J-R curves.

3.5 Crack length

Figure 5 shows the resulting J-R curves for

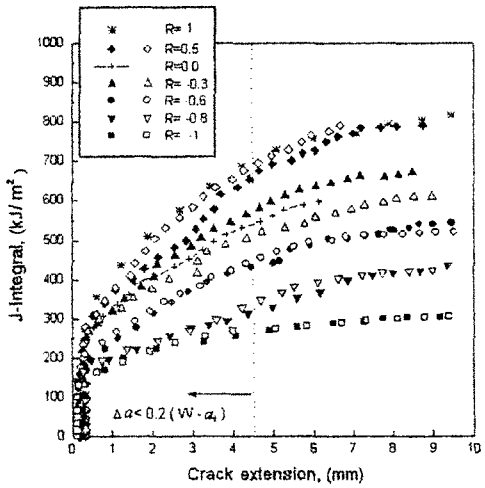

Fig. 6 Effect of Load Ratio on the Fracture Resistance Curve of SA516 Gr.70 Steel.

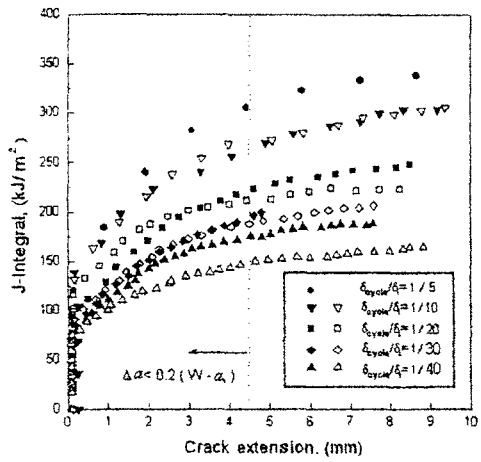

Fig. 7 Effect of Incremental Plastic Displacement on the Fracture Resistance Curve of SA516 Gr. 70 Steel.

various crack length to width ratio, a/W. The ASTM E1152-87 restricts the range for a/W from 0.5 to 0.75. It is because a specimen with a/W higher than 0.75 does not have enough crack ligament for the crack growth, and a specimen with a/W less than 0.5 produces insufficient constraint at the crack tip to result in a lower bound fracture toughness. In the present test, the a/W was changed from 0.25 to 0.85 a/W with an interval of 0.1. Except for a specimen with $a/W=0.25-B$, J-R curves decreased with increasing a/W.

4. Effect of Reverse Cyclic Loading

4.1 Load ratio

The experimental results for various load ratio were presented in Fig. 6 in terms of J-integral with increasing crack extension. The resulting J-R curves show that the J values are significantly reduced with decreasing the load ratio in the range of $\Delta a<0.2(W-a_i)$, where W denotes specimen width and a_i denotes the initial crack length. However, the decrease in the fracture resistance curve between $R=1$ and $R=0.5$ was not evident. This result proves the validity of ASTM E1152 requirement that restricts the amount of unloading up to 50% of the current maximum load.

4.2 Incremental plastic displacement

The resulting fracture resistance curves for various IPD were presented in Fig. 7. The resulting J-R curves showed a decreasing tendency of J-integral values with decreasing the δ_{cycle}/δ_i in the range of $\Delta a<0.2(W-a_i)$. In particular, the J-R curves considerably decreased when the δ_{cycle}/δ_i value changed from 1/5 to 1/20.

5. Discussion

5.1 Constraint effect

The behavior of the effect of specimen size as shown in Fig. 1 agrees to the effective range for J-R curve specified in ASME 813-89. Link (1991) reported that the change of size for A508 steel was not significant on J-R curve. The present A515 Grade 60 steel also showed no significant difference by changing the specimen size until the crack extension reached 3 *mm*. 1T -CT specimens, which are popular for general J-R curve test, produced lower bound J-R curves with sufficient crack extension.

The effect of plane size as shown in Fig. 2 implies that the increase of plane size without increasing thickness reduces the crack tip constraint; as the result of it, the higher J-R curves are obtained. 3PT-CT specimens showed slightly higher J-integral values than those for 2PT-CT specimens, however, the difference was trivial for

entire crack extension. No proportional relation between plane size and J-R curves was observed. Authors tested 1PT-CT and 4PT-CT specimens with A312 TP347 steel, and observed that 4PT -CT specimens recorded 3 times higher J-integral values compared to those for 1PT-CT specimens at the crack extension of $0.1b_o$ (b_o: uncracked ligament) on the previous study (Jo, et al. 1994). While 2PT-CT specimens showed about 2 times higher J-integral values than 1PT-CT, 3PT-CT specimens produced about 2.5 times higher J-integral values at $0.1b_o$. This trend is reasonable in comparison with the author's previous result (Jo, et al. 1994). However, the experimental data were not sufficient to derive a quantitative relation.

In general, a thicker specimen creates higher constraint at the crack-tip simulating plane strain condition. However, no significant difference was observed for various thickness specimens as shown in Fig. 3. Since all the specimens were side grooved, shear-lips at both surfaces were not formed, and thus the crack-tip satisfied the plane strain condition. Specimens with thickness of 12.7 *mm* (0.5 *inch*) produced lower bound J-R curves. While a 12.7 *mm* (0.5 *inch*) specimen gives a smallest net-section area (10.2 *mm*×45.7 *mm*), it may produce high constraint from 3 surfaces including two side grooved faces. These highly constrained sides may produce high hydrostatic stresses at the net-section area. The rate of a highly constrained area from the net -section area is relatively higher for a 12.7 *mm* (0.5 *inch*) thick specimen than other thick specimens. Lai and Ferguson (1986) reported that fracture toughness increases with decreasing specimen thickness until the thickness reaches a certain value satisfying plane strain condition for Comsteel En 25. They observed no significant difference with increasing specimen thickness after that point. J-R curves obtained from the present study show no significant difference for all cases implying that all side grooved specimens produced the plane strain condition at the crack -tip.

The size of shear-lip observed in the present test was about 30% of the thickness. Authors reported that the side groove effect was obvious for carbon steel but trivial for stainless steel on the previous study (Jo, et al. 1994). The present result shows that the fracture toughness of A515 Grade 60 steel is sensitive to side grooves. But no quantitative relation was available from the empirical data.

O' Dowd and Shih (1992) observed the effect of a/W on the crack-tip constraint, and proposed the J-Q approach in order to quantify such constraint effects. They reported that decreasing a/W decreased crack-tip constraint and resulted in lower hydrostatic stress at the crack-tip. The present test shows a good agreement with O' Dowd and Shih's (1992) results in terms of constraint. Since the specimen with lower constraint produces higher J-integral values, the decreasing tendency observed from J-R curves with increasing a/W implies the increase of crack -tip constraint. It is recommended that one study this constraint effect by applying finite element analysis.

5.2 Effect of load ratio

After J-R test under varied load ratios and incremental plastic displacements, micro Vickers hardness was measured at various positions perpendicular to the crack advancing surfaces of the test specimens. As seen in Fig. 8, the hardness values near the crack surface are larger for load ratio of 1 than for monotonic loading at constant

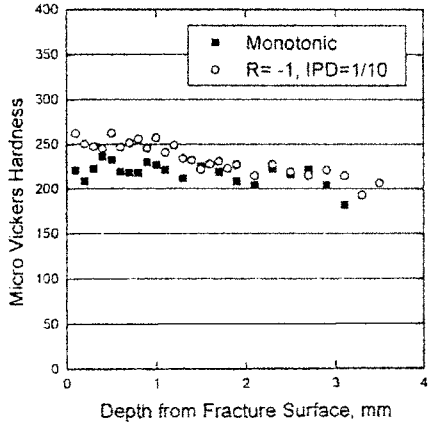

Fig. 8 Effect of Load Ratio on the Strain-Hardening Degree.

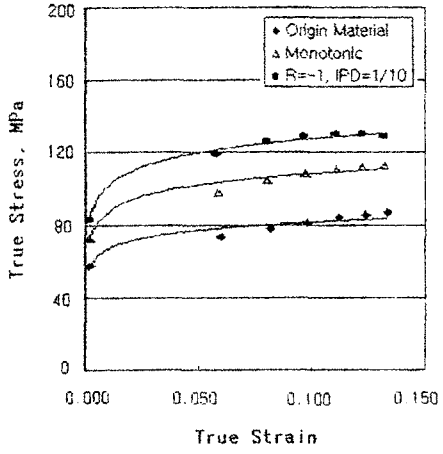

Fig. 9 Effect of Load Ratio on the True Stress- True Strain Curve.

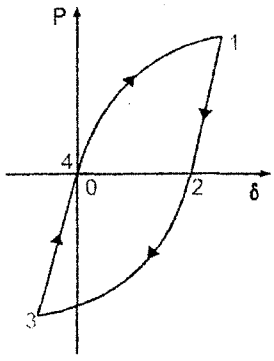

Fig. 10 Hysteresis Loops for Cyclic Loading.

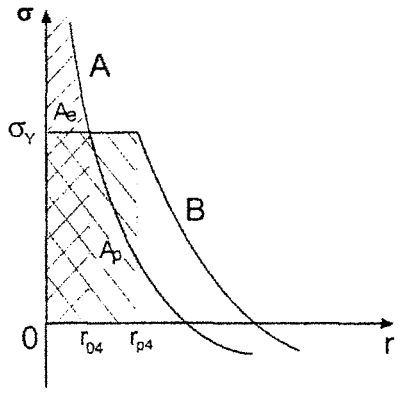

Fig. 11 Stress Distribution of a Crack Tip at Point 4.

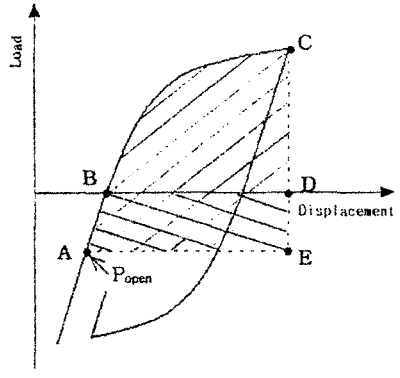

Fig. 12 Definition of Area for J Calculation under Reversed Cyclic Loading.

IPD (1/10). It is to be noted that the hardness is essentially the same below the surface increases (Fig. 8). Therefore, smaller R-values seem to result in increased hardening at the crack tip. Automated Ball Indentation (hereafter ABI) tests were also performed on non-strain-hardened original material and the J-R tested specimens using in-situ Stress-Strain Microprobe System procured from ATC (Haggag 1993; Haggag and Murty 1996). The ABI-derived true stress-true strain curves are shown in Fig. 9 illustrating the effects of load-ratio (R). As it is clear from the figure, strain-hardening increases following monotonic loading which further increased due to the reversed cyclic loading. From the hardness and the ABI tests, it was shown that decreased load ratio(R) leads to more strain-hardening at the crack tip. Thus the fracture toughness is expected to decrease as seen in Fig. 6.

From the stress field analysis near the crack tip of a compact tension fracture toughness test specimen, a cycle of tensile and compressive loads (Fig. 10) is seen to result in tensile residual stresses (B in Fig. 11, which did not exist at the crack tip before). Thus smaller loads are needed to advance the crack in the J-R tests following RCL. Consequently, the J-integral value will decrease. The tensile residual stress increased with the number of cycle and the residual stress is one of reasons of decreasing the J-R curves under the reversed cyclic loading.

From the stress field analysis near the crack tip of a compact tension fracture toughness test specimen, residual stress condition at point 3 in Fig. 10 was compression, however, residual stress condition at point 4 in Fig. 8 was tension as shown in

Fig. 11. It means that there is a neutral point at which the residual stresses is a zero between point 3 and point 4 in Fig. 10. From the point, the crack would be open while the specimen is still compressive loading condition. In general, the value of J-integral is measured from the load vs. load-line displacement curve. For the monotonic loading, the area defined as $S_{(BOD)}$ in Fig. 12 is used for the J-integral calculation. However, the phenomenon of crack opening and crack closure those are observed from the reversed cyclic loading tests is quite different that from the monotonic loading tests as illustrated in Fig. 12. While the crack opening is occurred at point B for the monotonic loading, it occurred at point A for the reversed cyclic loading condition. Therefore, the value of J-integral which is the actual energy consumed with crack growth must be measured from the area specified as $S_{(ABCDE)}$ covering the point P_{open}, the crack opening point (Dowling 1976; Dowling and Begley 1976), rather than $S_{(BCD)}$. In other words, calculating the J-integral for the reversed cyclic loading based on the area $S_{(BCD)}$ will underestimate the J-integral which should consider the area $S_{(ABDE)}$ to account for the effect of the reversed cyclic loading (Weon and Seok 1999). It will be one of reasons of decreasing the J-R curves under the reversed cyclic loading.

5.3 Effect of incremental plastic displacement

Increased IPD resulted in higher strain hardening but with increased J-R curve. It might be concluded that the J-R curve variation is dependent not on the strain hardening of the material but on the cyclic effect resulting in an increase of tensile residual stress. As shown in Fig. 13, the load line displacement of the IPD=1/5 specimen ($\delta_{1/15}$) for one cycle is same as that of the IPD=1/40 specimen ($\delta_{1/40}$) for 8 cycles. It means that the load was applied 8 times repeatedly for the IPD=1/40 specimen while the load was applied once for the IPD=1/5 specimen for the same J-integral value. The crack extension (Δa) for 1/5 specimen is larger than that for 1/40 specimen following one cycle of loading. However, the

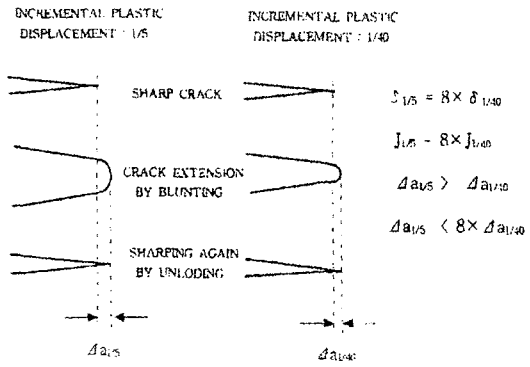

Fig. 13 Cycle Effect for Incremental Plastic Displacement Variation.

experimental measurements showed smaller crack extensions following 10 cycles in 1/5 specimen compared to that following 80 cycles in 1/40 specimen. The effect of decrease in IPD resulting in decreased J-R curves is due to fatigue. The tensile residual stress at the crack tip increases with the number
of cycles and thus can reduce the needed crack-advancing load that makes the J-R curves smaller.

6. Conclusions

(1) The resulting J-R curves showed that the effects of a/W and plane size on the J-R curve were significant. However, relatively weak influence was observed from the change of specimen thickness and size. The resulting J-R curves increased with increasing plane size and decreased with increasing a/W. It was also observed that the J-R curve decreased by applying the side grooves.

(2) The J-R curves under the reversed cyclic loading were affected by load ratio (R) and incremental plastic displacement (δ_{cycle}/δ_i). The J-R curves were decreased with decreasing the load ratio and the incremental plastic displacement, respectively. When the load ratio was set to -1, the resulting J-R curves were about 40~50 percent of those for the monotonic loading condition. Also on condition that the incremental plastic displacement reached 1/40, the J-R curves were about 50~60 percent of those for the

incremental plastic displacement of 1/10.

(3) For the fracture toughness specimen under the reversed cyclic loading, the strain hardening of the crack tip zone is increased with the decrease of load ratio. It was found that the tensile residual stresses are generated near the crack tip after the applied compressive load is removed and the tensile residual stress is increased as the number of cycle is increased. The strain hardening and the tensile residual stress make the fracture resistance values lower.

Acknowledgements

The authors are grateful for the support provided by a grant from the Korea Science & Engineering Foundation (KOSEF) and Safety and Structural Integrity Research Center at the Sungkyunkwan University.

References

Kirk, M.T., Koppenhoefer, K.C. and Shih, C. F., 1993, "Effect of Constraint on Specimen Dimensions Needed to Obtain Structurally Relevant Toughness Measures," *ASTM STP 1171*, pp. 79~104

Theiss, T. J. and Bryson, J. W., 1993, "Influence of Crack Depth on the Fracture Toughness of Reactor Vessel Steel," *ASTM STP 1171*, pp. 104~119

Joyce, J. A., Hackett, E. M. and Roe, C., 1993, "Effect of Crack Depth and Mode of Loading on the J-R Curve Behavior of a High-Strength Steel," *ASTM STP 1171*, pp. 239~263

Scott, P., Kramer, G., Vieth, P., Francini, R. and Wilkowski, Gery M., 1994, "The Effect of Dynamic and Cyclic Loading During Ductile Tearing on Circumferentially Cracked Pipe: Experimental Results," *ASME PVP* Vol. 280, pp. 207~220

Wilkowski, Gery M., Kramer, G., Vieth, P., Francini, R. and Scott, P., 1994, "The Effect of Dynamic and Cyclic Loading During Ductile Tearing on Circumferentially Cracked Pipe: Analytical Results," *ASME PVP* Vol. 280, pp. 221~239

Miura, Naoki Kashima, Koichi, Miyazaki, Katsumura and Kanno, Satoshi, 1997, "Effect of Negative Stress Ratio on Crack Growth for Cracked Pipe Subjected to Cycle Loading with Large-Scale Yielding," *ASME PVP*-Vol. 350, Fatigue and Fracture 1, Book No. G01062

Miura, Naoki, Fujioka, Terutaka, Kashima, Koichi, Kanno, Satoshi, Hayashi, Makoto, Ishiwata Masayuki, and Gotch, Nobuho, 1993, "Evaluation of Dynamic Fracture Strength for Japanese Carbon Steel Pipes," Komae Research Laboratory

Choi, Y. H., 1995, IPIRG-2 Program Visiting Scientist Reports, KINS

Seok, C. S., Kim, Y. J., and Weon, J. I., 1998, "Effect of Reverse Cyclic Loading on the Fracture Resistance Curve in C(T) Specimen," 2nd International Workshop on The Integrity of Nuclear Components, pp. 249~257, The Japan Welding Engineering Society Atomic Energy Research Committee

ASTM E813-89, 1996, "Standard Test Method for JIC, A Measure of Fracture Toughness," Annual book of ASTM standards, pp. 646~660

ASTM E1152-95, 1996, "Standard Test Method for Determining J-R Curves," Annual book of ASTM standards, pp. 763~773

Link R. E., and Lander, J. D., 1991, "Something new on size and constraint effects for J-R curves," *Mechanical Engineering Publications*, London, pp. 707~721

Y. J. Jo, Y. J. Kim and C. S. Seok, 1994, "A Study on the Crack Tip Constraint Effect for Fracture Resistance Curves," *Proceedings of the KSME Autumn Annual Meeting I*, pp. 42~46

Lai M. O., and Ferguson, W. G., 1986, "Effect of Specimen Thickness on Fracture Toughness," *Engineering Fracture Mechanics*, Vol. 23, No. 4, pp. 649~659

O' Dowd N. P., and C. F. Shih, 1992, "Family of Crack-Tip Fields Characterized by a Triaxiality Parameter," *Journal of Mechanics and Physics of Solids*, Vol. 40, pp. 939~963

Haggag Fahmy M., 1993, "In-Situ Measurements of Mechanical Properties Using Novel Automated Ball Indentation System," Small Specimen Test Techniques Applied to Nuclear Reac-

tor Vessel Thermal Annealing and Plant Life Extension, ASTM STP1204, pp. 27~44

Haggag Fahmy M., and Murty K. L., 1996, "A Novel Stress-Strain Microprobe for Non-destructive Evaluation of Mechanical Properties of Materials," Proceedings of Non-destructive Evaluation and Materials Properties Ⅲ, TMS Fall Meeting, pp. 101~106

Dowling, N. E., 1976, "Geometry Effects and the J-Integral Approach to Elastic-Plastic Fatigue Crack Growth," ASTM STP 601, pp. 19~32

Dowling, N. E., and Begley, J. A., 1976, "Fatigue Crack Growth During Gross Plasticity and the J-Integral," Mechanics of Crack Growth, ASME STP 590, pp. 82~103

Weon, Jong Il and Seok, Chang Sung, 1999, "Effect of Reverse Cyclic Loading on the Fracture Resistance Curve of Nuclear Piping Material," Transactions(A) of the KSME, Volume 23, No. 7, pp. 1112~1119